Real-time seismic structural response prediction system based on support vector machine

Kuang Yi Lin[a], Tzu Kang Lin[*] and Yo Lin[b]

Department of Civil Engineering, National Chiao Tung University, 1001 University road, Hsinchu 300, Taiwan, ROC

Abstract.   Floor acceleration plays a major role in the seismic design of nonstructural components and equipment supported by structures. Large floor acceleration may cause structural damage to or even collapse of buildings. For precision instruments in high-tech factories, even small floor accelerations can cause considerable damage in this study. Six P-wave parameters, namely the peak measurement of acceleration, peak measurement of velocity, peak measurement of displacement, effective predominant period, integral of squared velocity, and cumulative absolute velocity, were estimated from the first 3 s of a vertical ground acceleration time history. Subsequently, a new predictive algorithm was developed, which utilizes the aforementioned parameters with the floor height and fundamental period of the structure as the new inputs of a support vector regression model. Representative earthquakes, which were recorded by the Structure Strong Earthquake Monitoring System of the Central Weather Bureau in Taiwan from 1992 to 2016, were used to construct the support vector regression model for predicting the peak floor acceleration (PFA) of each floor. The results indicated that the accuracy of the predicted PFA, which was defined as a PFA within a one-level difference from the measured PFA on Taiwan's seismic intensity scale, was 96.96%. The proposed system can be integrated into the existing earthquake early warning system to provide complete protection to life and the economy.

Keywords: Support Vector Machine (SVM); Support Vector Regression (SVR); p-wave features; Peak Floor Acceleration (PFA); earthquake early warning; seismic hazard mitigation; reduced-scale model

1. Introduction

Earthquakes cause damage to structures, facilities in structures, and nonstructural components. Damage after earthquakes can affect the function of structures (Kanee *et al.* 2013), which is a major concern. According to Rodriguez *et al.* (2002), earthquake-induced damage to nonstructural components may cause the structure to collapse. Moreover, precision instruments used in high-tech factories can be affected by even a small-scale earthquake. The estimation of floor acceleration on structures is critical in predicting the seismic performance of nonstructural component commonly installed in building.

The seismic design of equipment supported by structures depends on the floor acceleration response spectrum (Calvi and Sullivan 2014), which is different from the seismic design of buildings itself. Floor acceleration is affected by the dynamic amplification of a structure. The degree of amplitude and frequency concentration depends on the floor height. In general, a greater floor height is associated with a higher amplitude and higher frequency concentration. Floor acceleration has an amplification effect with floor elevation, and a high-rise structure could exhibit resonance effects during long-period earthquakes (Kubo *et al.* 2011, Takabatake and Ikarashi 2013, Loi *et al.* 2016). Such acceleration have been responsible for inertia force causing damage to services and are a major reason for structural damage and even building collapse (Rodriguez *et al.* 2002). Therefore, evaluating the response of floor acceleration is crucial. All current earthquake early warning systems (EEWSs) focus only on the prediction of peak ground acceleration (PGA); however, from a structural perspective, peak floor acceleration (PFA) is more important than PGA. PFA affects the operation of equipment and nonstructural components in structures. Therefore, an early warning system for PFA must be established to ensure the safety of nonstructural components of structural systems, provide emergency response measures, and shut down precision instruments in high-tech factories in order to reduce the destructiveness of earthquakes.

An EEWS utilizes the different propagation speeds of seismic waves in an earthquake. Seismic waves can be categorized into three types, namely P-, S-, and surface waves. Surface waves have the largest amplitude, followed by S- and P-waves. Surface waves and S-waves cause large-scale destruction. Although P-waves have the smallest amplitude, they are faster than S-waves and surface waves. Therefore, an EEWS can predict seismic waves that cause large-scale destruction and can issue early earthquake warnings by monitoring P-waves.

An EEWS can be classified into two models according to the applied methodology (Kanamori 2005): regional

---

*Corresponding author, Associate Professor
  E-mail: tklin@nctu.edu.tw
[a]Ph.D. Student,
  E-mail: kuangyi.cv02g@nctu.edu.tw
[b]Master,
  E-mail: joelin04170@gmail.com

warning and on-site warning models. In the regional warning model, a seismic observation network is constructed in a region with frequent earthquakes. When an earthquake occurs, the network collects real-time data from the station group near the epicenter to determine the location, scale, and impacts of the earthquake. A warning is then sent to the area where the S-wave has not yet arrived. However, this model has a considerably large blind zone radius: at an S-wave velocity of 3 km/s, the release time is approximately 20-30s; that is, the epicenter radius is at least 60 km, which is the radius of the alarm blind zone. Therefore, processing the data to provide a prompt warning requires a considerably long time. The on-site warning model uses P-wave information to estimate the earthquake magnitude before the S-wave arrives and then issues an alarm. Although its accuracy is lower than that of regional warning, the radius of the alarm blind zone can be considerably reduced (considering the 3 s P-wave information, if the focal depth is 5 km, the alarm blind zone radius can be reduced to approximately 20 km). In Taiwan, the epicenters of most earthquakes are located in high-population-density areas; therefore, the development of on-site warning systems in terms of narrowing the alarm blind zone is crucial.

The National Center for Research on Earthquake Engineering (NCREE) has developed a real-time warning system for strong earthquakes (Tsai 2010). When the ratio of the short-term average to long-term average exceeds a user-defined threshold, the monitoring system is triggered and predicts the PGA of the vibration events. If the predicted PGA is larger than 25 gal (magnitude-4 earthquake on Taiwan's seismic intensity scale) or the monitored PGA is larger than a defined threshold, the system issues an alarm (Fig. 1). Currently, there exist two empirical regression formulas for prediction, namely PGA prediction developed by the NCREE and the method of Hsu et al. (2013); however, both methods cannot predict PFA.

Lin and Wu (2017) used support vector regression (SVR) for PFA prediction. They selected the PGA over 250 gal of earthquake events (magnitude-6 earthquakes on Taiwan's seismic intensity scale), which were monitored by the Structure Strong Earthquake Monitoring System (SSEMS) of the Central Weather Bureau (CWB) in Taiwan, and extracted the features of the first 10 s of the P-wave. The accuracy of the predicted PFA, located within a one-level difference on the seismic intensity scale from the real PFA, was 95.51%.

To improve accuracy, this study increased the amount of seismic data and reduce the extraction time to 3 s. In addition, a reduced-scale model was designed for shake table testing to establish a customized PFA prediction model that can provide adequate early warning for buildings. The study process is displayed in Fig. 2.

2. Research methods

2.1 P-wave features

Wu (2005) and Wu and Zhao (2006) have indicated that
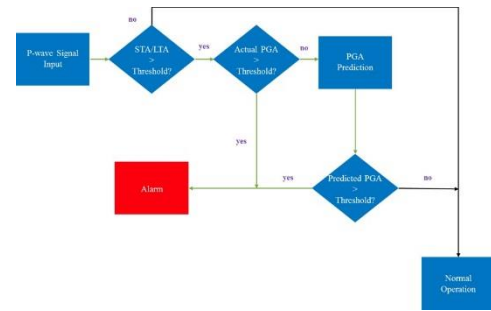

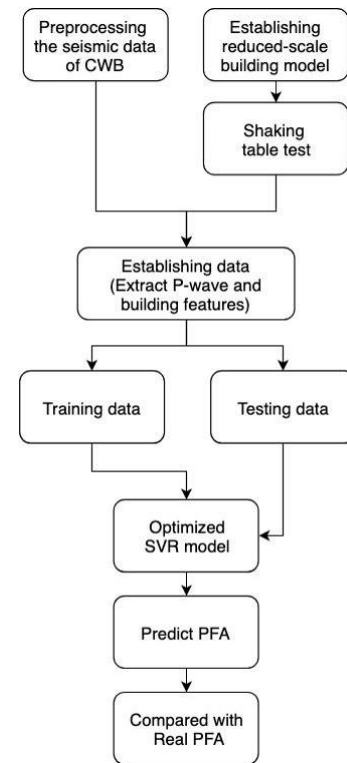Fig. 1 Theory of on-site EEWS

Fig. 2 Research structure

a larger earthquake is associated with a longer vibration period of seismic signals. In other words, the scale of magnitude of an earthquake can be estimated from the vibration period of the P-wave. According to Satriano et al. (2011), the P-wave features used by an EEWS include peak measurements, integral quantities, the predominant period, and the average peak. The calculation of integral quantities is explained in the paper of Böse et al. (2012).

To predict PFA, the system extracts the building height, natural period of the structure, and vertical acceleration of the first 3 s of the P-wave captured by a single observation station. Thus, eight parameters are considered, namely the effective predominant period (Tc), peak acceleration (Pa), peak velocity amplitude (Pv), peak displacement amplitude (Pd), cumulative absolute velocity (CAV), integral of squared velocity (IV2), building height, and natural period of the structure. These parameters are used as input items to train and test SVR model for predicting PFA.

Among the eight parameters, Pa, Pv, and Pd are indirectly relevant to PGA, peak ground velocity, and peak

ground displacement. According to Kanamori (2005), there exists a relationship between Tc and earthquake magnitude; that is, the larger an earthquake is, the longer the vibration period of the seismic signal is. IV2 also depends on the earthquake's magnitude, and CAV can be used to determine the destructiveness of an earthquake.

The effective predominant period (Tc), CAV, and integral of squared velocity (IV2) can be calculated as follows

$$T_c = \frac{2\pi}{\sqrt{r}} \quad , where \quad r = \frac{\int_0^{t_p} \dot{u}(t)^2 dt}{\int_0^{t_p} u(t)^2 dt} \tag{1}$$

$$IV2 = \int_0^{t_p} \dot{u}(t)^2 dt \tag{2}$$

$$CAV = \int_0^{t_p} |\ddot{u}(t)| dt \tag{3}$$

where $u(t)$, $\dot{u}(t)$, and $\ddot{u}(t)$ are the vertical components of displacement, velocity, and acceleration time histories of ground motion after P-wave arrival, respectively.

To calculate P-wave features, acceleration data of earthquakes are integrated to obtain the velocity and displacement. This study used a high-pass filter to correct for bias shifting at low frequency, where the order and cutoff frequency of the filter were determined to be 2 and 0.075 Hz, respectively.

2.2 Support vector regression

Support vector machine (SVM) is a type of machine learning based on statistical learning theory, which can efficiently deal with a small sample size. Support vector regression (SVR) achieves a compromise between model complexity, learning ability, and generalization ability (Zhang *et al.* 2014). SVR is an SVM algorithm used to solve regression.

SVR can be projected to a higher dimensional feature space H by a nonlinear projection function, and the precise outcome can be predicted easily. With this, the linear regression function can be expressed as follows

$$y = f(x) = w \cdot \phi(x) + b \ \ with \ \ w \in x, b \in \mathbb{R} \tag{4}$$

where w is a regression coefficient vector in the feature space, ϕ is the nonlinear mapping function for projection, and b is the model offset (Zhang *et al.* 2014).

Consider the following training set

$$\{(x_1, y_1), \cdots, (x_\ell, y_\ell)\} \ with \ x \in \mathbb{R}^d, y \in \mathbb{R}, i = 1, \cdots, \ell \tag{5}$$

x_i and y_i are input variable vector and output variable vector respectively.

If the error between $f(x_i)$ and y_i is less than the error tolerance ε for each x_i, then $f(x)$ can predict y correctly from x. Thus, w is the optimal separating hyperplane of SVR.

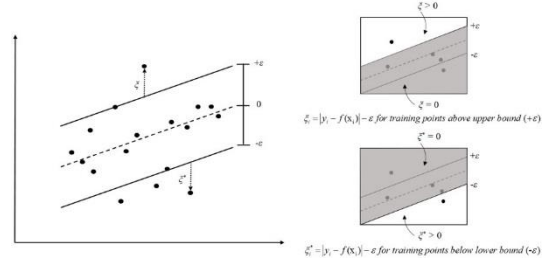Data are occasionally affected by noise and errors. The quality of estimation is measured by Vapnik's ε-insensitive

Fig. 3 A schematic diagram of SVR using Vapnik's ε-sensitive loss function

loss function $L(y, f(x))$ (Vapnik 2013)

$$L(y, f(x)) = \begin{cases} 0 & if \ |y_i - f(x)| \le \varepsilon \\ |y_i - f(x)| - \varepsilon & otherwise \end{cases} \tag{6}$$

The goal in using the ε-insensitive loss function is to find a function that fits the current training data with a deviation less than or equal to ε. That is, the loss is zero if the difference between the predicted $f(x)$ and the observed value y is less than ε; otherwise, the loss is given by the absolute difference between these two values. Thus, Vapnik's ε-insensitive loss function defines a radius ε (see Fig. 3) around the target values y. Then, it follows that

$$\xi_i = |y_i - f(x_i)| - \varepsilon \tag{7}$$

"for training points above upper bound "(+ε)

$$\xi_i^* = |y_i - f(x_i)| - \varepsilon \tag{8}$$

"for training points below lower bound "(-ε)

where ξ_i and ξ_i^* are slack variables for the mutually exclusive situations presented in (7) and (8).

Fig. 3 illustrates SVR method and Vapnik's ε-sensitive loss function. The system must compromise between border width and decision boundary. The range of the radius tolerance ε is related to the data. The data on the line or out of the boundary are called support vectors (i.e., vectors of the data trend).

The regression problem can be expressed as the following constrained optimization problem (Schölkopf *et al.* 2000)

$$\min_{w,b,\xi_i,\xi_i^*} \left[\frac{1}{2} \|w\|^2 + C \cdot \left(v\varepsilon + \frac{1}{\ell} \sum_{i=1}^{\ell} (\xi_i + \xi_i^*) \right) \right] \tag{9}$$

$$subject \ to \ \begin{cases} w \cdot \phi(x_i) + b - y_i \le \varepsilon + \xi_i \\ y_i - (w \cdot \phi(x_i) + b) \le \varepsilon + \xi_i^* \\ \xi_i, \xi_i^* \ge 0 \ for \ i = 1, \dots, \ell \end{cases}$$

where ℓ is the number of training data, C is a positive constant that determines the degree of penalized loss when a training error occurs, and v is a lower bound on the fraction of support vectors.

Introducing the method of Lagrange multipliers and setting the Lagrange multipliers α_i and β_i, lead to the transformation of the objective function into a dual problem

$$\max_{\alpha,\beta} \left[\sum_{i=1}^{\ell} y_i(\alpha_i - \beta_i) \right] \tag{10}$$

$$-\frac{1}{2}\sum_{i=1}^{\ell}\sum_{j=1}^{\ell}(\alpha_i-\beta_i)(\alpha_j-\beta_j)\,k(x_i,x_j)\Bigg]$$

$$subject\ to \begin{cases} \sum_{i=1}^{\ell}(\alpha_i-\beta_i)=0 \\ \beta_i\in\left[0,\dfrac{C}{\ell}\right] \\ \sum_{i=1}^{\ell}(\alpha_i-\beta_i)\le C\cdot v \end{cases}$$

In the preceding function, α_i and β_i ($i=1,2,...,m$) represent Lagrange multipliers and $k(x_i,x_j)$ represents the kernel function, which is adopted as a radial basis kernel function as follows

$$k(x_i-x_j)=exp\left(-\frac{\|x_i-x_j\|^2}{2\sigma^2}\right),where\ \ \frac{1}{2\sigma^2}=\gamma \quad (11)$$

The quadratic programming problem is used to determine the Lagrange multipliers α_i and β_i. Then, the parameters w and b can be estimated under the Karush-Kuhn-Tucker complementarity conditions (Fletcher 2013). Therefore, the prediction function can be expressed as follows

$$f(x)=\sum_{i=1}^{j}(\alpha_i-\beta_i)\,k(x_i,x_j)+b \quad (12)$$

where j is the number of nonzero terms.

The grid search method was applied to determine the optimal values of C and γ in this study, where the ranges of C and γ were 2^5 to 2^{15} and 2^{-12} to 2^{-1}, respectively. The obtained model was determined as the optimal model.

2.3 Earthquake time history database

This study was divided into two phases for the establishment of the prediction model. In the first phase, a generic prediction model was established through the signal data collected by the SSEMS for 39 buildings settled by the Taiwan CWB. The second phase involved establishing a customized prediction model. This study designed a reduced-scale model to replace the real structure. Furthermore, a shaking table test was performed to expand the earthquake time history database. The databases obtained in the two phases are described in the following text.

2.3.1 Time history database of the generic prediction model

Since 1992, the CWB has established the SSEMS under the Taiwan Strong Motion Instrumentation Program. The SSEMS collects data from accelerometers installed in
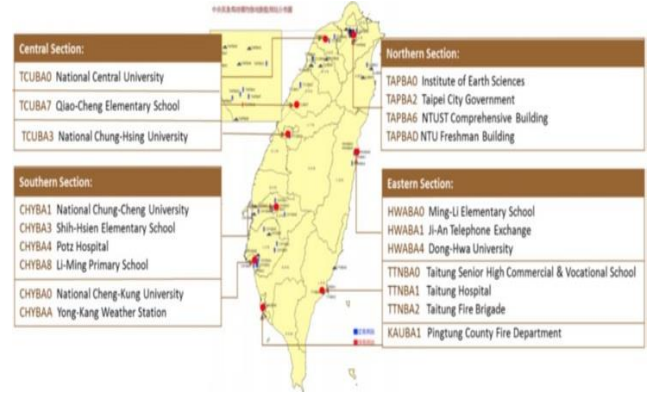

Fig. 4 Locations of the 20 selected station structures

39 buildings in Taiwan. The sample frequency of each data set is 200 or 250 Hz, and the resolution is typically 16 bits.

In this study, 20 buildings were selected (Fig. 4) and 4,692 pieces of seismic data collected from 1992 to 2016 were used.

2.3.2 Time history database of the customized prediction model

Due to the high cost involved, every building could not afford the SSEMS. Therefore, a customized PFA prediction model was difficult to achieve. To overcome this problem, the time history acceleration of a representative earthquake was input into a reduced-scale model of the structure. A shaking table test was performed with the input to obtain the seismic data of each floor of the simulated structure.

Subsequently, the result was input into the generic prediction model established in the first phase to obtain the customized PFA prediction model.

2.3.3 Shaking table test of the reduced-scale model

The proportion of the reduced-scale model to an imaginary structure, which was based on the administration building in the Central Taiwan Science Park was determined to be 1:33. The structure is composed of 9- and 13-story buildings, and the first to third floors of the two buildings are joined together. The results obtained are expected to be applicable to a wide range of structures.

Structural elements can be divided into three types, namely beam, column, and floor slab elements, which affect the structural dynamic characteristics. The reduced-scale example was constructed under three limitations: dimension of the shaking table: 2500 mm × 1200 mm; steel table weights: 800 kg; and load carrying capacity: 1000 kg. The twin-tower reduced-scale model was a combination of the 9- and 13-story buildings, and each floor measured 1000 mm (L) × 697 mm (W) × 135 mm (H). The three-story structure connected the two buildings and measured 300 mm (L) × 697 mm (W) × 135 mm (H). In general, the model was 2300 mm long and 697 mm wide.

To reduce the weight of the reduced-scale model, aluminum alloy was used as the beam material and medium-carbon steel S45C was used for the columns (Fig. 5). The high rigidity of the aluminum alloy could prevent the deformation of the plate.

Fig. 5 Reduced-scale model

Table 1 Similitude laws of the experiment

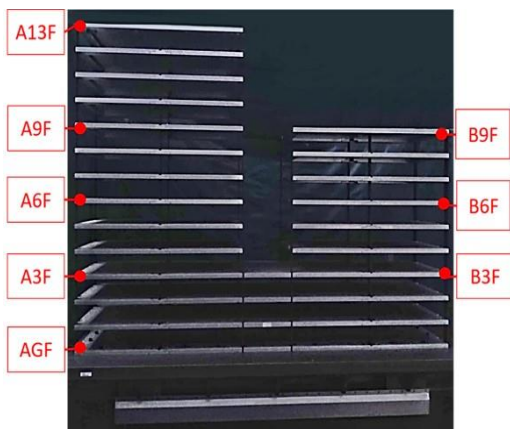| Physical property	Scale factor (from full-scale to model)
Length	$S_\ell = \dfrac{1}{33}$
Time	$S_t = S_\ell^{1/2} = 0.174$
Frequency	$S_\omega = S_\ell^{-1/2} = 5.74$
Acceleration	1

Fig. 6 Accelerometer layout in the twin-tower reduced-scale model

In this study, structural dynamic characteristics were determined through modal analysis. The first step was to ensure that the first natural frequency of the reduced-scale model was equal to the frequency of the original structure multiplied by the corresponding similitude law factor. The similitude law factor can be determined using scale theory proposed by Harris and Sabnis (1999). To simulate the PFA of each floor, artificial mass simulation was used as the basis for calculating transformations, and the scale factor of acceleration was 1.

The linear dimension factor was determined to be S_ℓ. During the execution of the shaking table experiment, the time scale factor was S_t. For determining the structural dynamic performance, the first natural frequency was used as a reference parameter (the frequency scale factor is $S\omega$). The aforementioned factors are presented in Table 1.

The scale model was based on the 13-story the administration building in the Central Taiwan Science Park. According to the empirical formula, the fundamental vibration period of a building is about one-tenth of the total number of floors. As a result, the first nature frequency of the actual building is approximately 0.80 Hz. When the frequency scale factor S_ω was set to 5.74, the theoretical nature frequency of the scale model was 4.59 Hz.

In addition, the shaking table test was conducted on the twin-tower reduced-scale model by inputting white noise and using FFT; a nearly similar natural frequency of 4.36 Hz was obtained.

Fig. 6 displays the locations of the accelerometers in the twin-tower reduced-scale model. In the twin-tower reduced-scale model, the two towers had a total of eight accelerometers. In tower A, the accelerometers were installed at GF, 3F, 6F, 9F, and 13F according to the configuration of the structure and the possible reaction of the structure during the earthquake. In tower B, the accelerometers were installed at 3F, 6F, and 9F. Digital signals were recorded with a sample frequency of 200 Hz.

The customized PFA prediction model was designed for creating a PFA warning system for the Central Taiwan Science Park. Fifteen earthquake events from 1992 to 2016 recorded by four observation stations located around the Central Taiwan Science Park, namely TCU057, TCU100, TCU105 and TCU060, were selected as training events. The earthquake events were magnified by different factors to obtain additional training and testing earthquake events. In total, 264 training samples were obtained from the 15 earthquake events. Representative Earthquake Data, which comprised 216 samples selected from TCU057, TCU100, and TCU105, were used to establish SVR model. Then, 48 samples from TCU060, which were called the Testing Earthquake Data, were used to inspect SVR model.

3. Analysis result

3.1 Testing result for the generic regression model

To apply SVR model, 75% of the 4692 pieces of data were randomly selected as the training data set and the radial basis function (RBF) was selected as the kernel function. The grid search method was used to determine the optimal cost parameter (C=2048) and kernel function parameter (γ=0.125). The squared correlation coefficient of the training regression model (R^2_{tr}) was 0.75884.

In order to make it easier to determine the degree of earthquake shaking, this study categorized the value of peak floor acceleration predicted by regression according to Taiwan's seven-tiered seismic intensity scale in Table 2. The

Table 2 Taiwan's seven-tiered seismic intensity scale
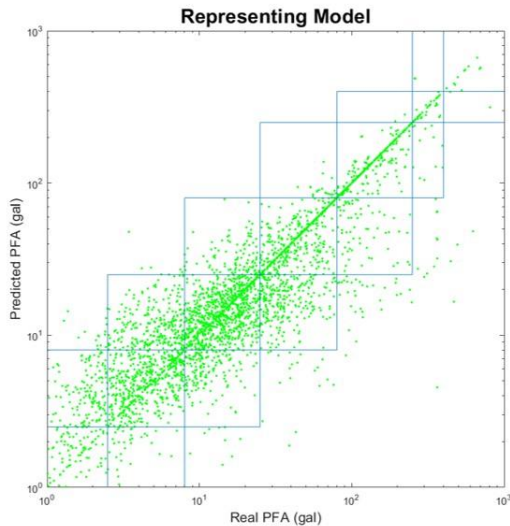
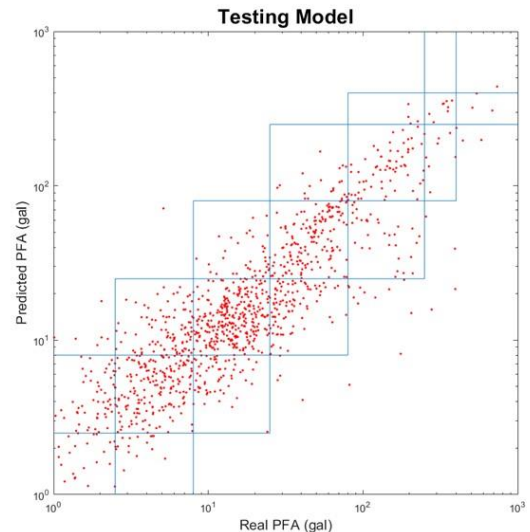| Intensity	0	1	2	3	4	5	6	7
Gal	<0.8	0.8-2.5	2.5-8	8-25	25-80	80-250	250-400	>400

Fig. 7 Result of the training regression model

Table 3 Comparison of the regression model in this study with the model of Lin and Wu (2017)

	The proposed regression model	Lin and Wu (2017)
Time to exact P-wave features	3 s	10 s
R^2_{tr}	0.75884	0.89813
R^2_t	0.69867	0.31962
Accuracy rate	97.02%	95.51%

* R^2_{tr}: squared correlation coefficient of the training regression model; R^2_t: squared correlation coefficient of the testing regression model

standard deviation between the predicted PFA and monitored PFA was 33.76 gal. The seismic intensity of the predicted PFA located within a one-level difference of the monitored PFA was considered as accurate. The accuracy rate was up to 96.96%. Fig. 7 depicts the result of the training regression model. The blue line represents the classification criterion of the CWB.

Moreover, when the remaining 25% of the database (1,173 samples) was input into the regression model, the squared correlation coefficient (R2t) was 0.69867, and the standard deviation between the predicted PFA and monitored PFA was 39.71 gal. The accuracy of the predicted PFA, located within a one-level difference of the seismic intensity scale from the monitored PFA, was 97.02%. Fig. 8 presents the results of the testing regression model.

Table 3 presents a comparison of the results with those of Lin and Wu (2017). When the number of seismic samples was increased, the time required for exacting P-wave features was effectively shortened and the accuracy of prediction was increased.

3.2 Testing result of the customized regression model

A total of 4,908 samples were collected from the generic prediction time database and the customized database

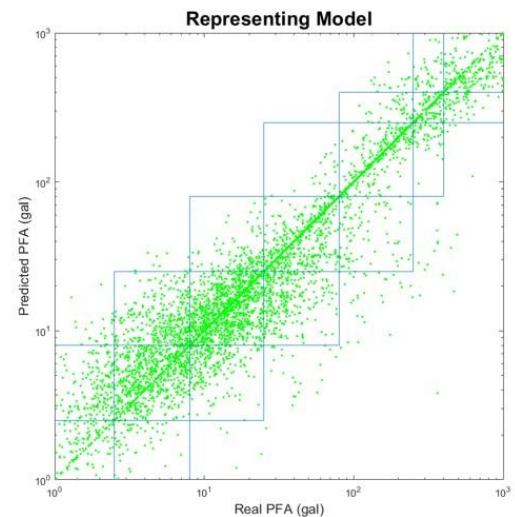Fig. 8 Result of the testing regression model

Fig. 9 Customized regression model

collected from the shaking table test. The RBF was taken as the kernel function, and the grid search method was applied to determine the optimal cost parameter (C) and kernel function (γ). The optimal cost parameter and kernel function were 2048 and 0.125, respectively. The squared correlation coefficient was 0.775114. The accuracy of the predicted PFA, located within a one-level difference on the seismic intensity scale from the monitored PFA, was 96.14%. Fig. 9 illustrates the results of the customized regression model. Comparing the generic training and customized regression models show as in Figs. 7 and 9, the accuracy of the prediction result was above 96.0% for both. In addition, a significant increase in the seven-tiered intensity can be observed in Fig. 9. The customized regression model included the samples of strong earthquakes.

To test the customized SVR model, 48 samples were selected for the shaking table test of six time history
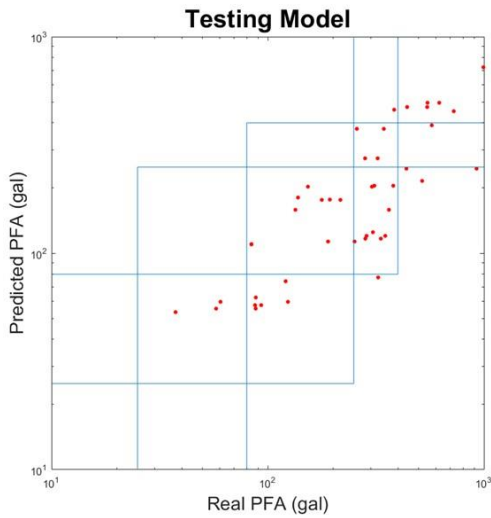
Fig. 10 Customized testing SVR model
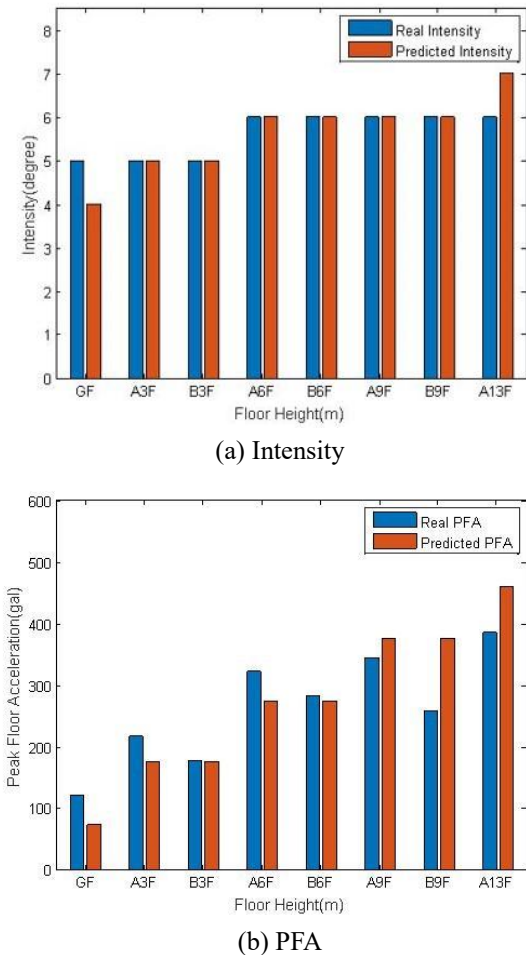

(a) Intensity

(b) PFA

Fig. 11 Comparison of the predicted and real result for TCU060-201600531-20

records from the TCU060 observation station. Fig. 10 illustrates the results obtained for the customized SVR model, whose squared correlation coefficient was 0.38777. The accuracy of the predicted PFA, located within a one-

level difference on the seismic intensity scale from the monitored PFA, was 81.25%. This thus demonstrates that a suitable customized PFA warning system can be developed.

Furthermore, this study selected the seismic acceleration time history obtained from the TCU060 observation station on May 31, 2016, as the actual PFA, which differed from the PFA predicted by the customized SVR model (Fig. 11).

The results indicated a high correlation between the predicted PFA and the height of the structure. Moreover, the trends of the predicted and monitored PFA were similar. However, some underestimation of the predicted PFA also occurred. The main reasons for this phenomenon may be that the EEWS extracts only the first few seconds of the P-wave and ignores the effect of long or complex slip propagation processes.

4. Conclusions

PFA is a critical parameter influencing the performance of nonstructural elements in buildings. This study developed two types of real-time predictive PFA models, namely generic and customized PFA models for individual buildings. The generic PFA model is based on SVR and uses six P-wave features extracted from the first 3 s of P-wave vertical acceleration at a single observation station. Structural parameters, including the floor height and fundamental period of the structure are also considered. The Representative Earthquake Data comprised 70% of the 4692 records obtained from 1,179 earthquake events that occurred during 1992-2016. To evaluate the accuracy of the PFA predictions, 30% of the 4,692 earthquake records were used as Testing Earthquake Data. Overall, the standard deviation between the predicted generic PFA and real PFA for the Testing Earthquake Data was 39.71 gal, and the accuracy of the predicted PFA, located within a one-level difference on the seismic intensity scale, from the real PFA was 97.02%. The study also indicated that the accuracy of shortening tp to 3 s was close to 10 seconds. In other words, the research results can provide increased reaction time before an earthquake.

A customized PFA model was established on the basis of the generic PFA model and a shaking table test of the reduced-scale model. Therefore, the customized PFA model can be said to optimize the generic PFA model for a specific structure. The accuracy of the predicted PFA, located within a one-level difference on the seismic intensity scale from the monitored PFA, was 81.25%. Nevertheless, the accuracy of the customized model is lower than the generic model. The main reason for this phenomenon may be that only a few databases were collected by the reduced-scale experiment for the customized PFA model. However, the feasibility of the customized PFA model can still be verified by considering the May 31, 2016, earthquake event recorded by the TCU06 seismic observation station. The predicted trend approximated the monitored PFA trend.

In this study, the customized evaluation of the PFA prediction model was achieved. The proposed method can enable people to prepare for danger and act before an

earthquake occurs. It also provides a valuable reference to engineers for structural health monitoring after an earthquake.

References

Böse, M., Heaton, T. and Hauksson, E. (2012), "Rapid estimation of earthquake source and ground-motion parameters for earthquake early warning using data from a single three-component broadband or strong-motion sensor", *Bull. Seismol. Soc. Am.*, **102**(2), 738-750. https://doi.org/10.1785/0120110152.

Calvi, P.M. and Sullivan, T.J. (2014), "Estimating floor spectra in multiple degree of freedom systems", *Earthq. Struct.*, **7**(1), 17-38. https://doi.org/10.12989/eas.2014.7.1.017.

Fletcher, R. (2013), Practical Methods of Optimization, John Wiley and Sons, New Jersey, U.S.A.

Harris, H.G. and Sabnis, G. (1999), Structural Modeling and Experimental Techniques, CRC press, Florida, U.S.A.

Hsu, T.Y., Huang, S.K., Chang, Y.W., Kuo, C.H., Lin, C.M., Chang, T.M., and Loh, C.H. (2013), "Rapid on-site peak ground acceleration estimation based on support vector regression and P-wave features in Taiwan", *Soil Dyn. Earthq. Eng.*, **49**, 210-217. https://doi.org/10.1016/j.soildyn.2013.03.001.

Kanamori, H. (2005), "Real-time seismology and earthquake damage mitigation", *Annu. Rev. Earth Plan. Sci.*, **33**, 195-214.

Kanee, A.R.T., Kani, I.M.Z. and Noorzad, A. (2013), "Elastic floor response spectra of nonlinear frame structures subjected to forward-directivity pulses of near-fault records", *Earthq. Struct.*, **5**(1), 49-65. https://doi.org/10.12989/eas.2013.5.1.049.

Kubo, T., Hisada, Y., Murakami, M., Kosuge, F. and Hamano, K. (2011), "Application of an earthquake early warning system and a real-time strong motion monitoring system in emergency response in a high-rise building", *Soil Dyn. Earthq. Eng.*, **31**(2), 231-239. https://doi.org/10.1016/j.soildyn.2010.07.009.

Lin, T.K., and Wu, C.H. (2017), "Estimation of peak floor acceleration based on support vector regression and p-wave features", MATEC Web of Conferences, 119. https://doi.org/10.1051/matecconf/201711901028.

Loi, D.W., Raghunandan, M.E. and Swamy, V. (2016), "Seismicity of peninsular Malaysia due to intraplate and far field sources", *Earthq. Struct.*, **10**(6), 1391-1404. https://doi.org/10.12989/eas.2016.10.6.1391.

Rodriguez, M.E., Restrepo, J.I. and Carr, A.J. (2002), "Earthquake-induced floor horizontal accelerations in buildings", *Earthq. Eng. Struct. D.*, **31**(3), 693-718. https://doi.org/10.1002/eqe.149.

Satriano, C., Wu, Y.M., Zollo, A. and Kanamori, H. (2011), "Earthquake early warning: Concepts, methods and physical grounds", *Soil Dyn. Earthq. Eng.*, **31**(2), 106-118. https://doi.org/10.1016/j.soildyn.2010.07.007.

Schölkopf, B., Smola, A.J., Williamson, R.C. and Bartlett, P.L. (2000), "New support vector algorithms", *Neural Cpmput.*, **12**(5), 1207-1245. https://doi.org/10.1162/089976600300015565.

Takabatake, H. and Ikarashi, F. (2013), "New vibration control device and analytical method for slender structures", *Earthq. Struct.*, **4**(1), 11-39. https://doi.org/10.12989/eas.2013.4.1.011.

Tsai, K.C., Lin, P.Y., Lin, C.C.J., Lin, T.K., Lin, Y.B., Lin, J.L., and Chung, C.S. (2010), "Preliminary study of added-value information and analysis for earthquake early warning system", *Nat. Center Res. Earthq. Eng.*, 9-13.

Vapnik, V. (2013), The Nature of Statistical Learning Theory, Springer science and business media, Berlin, Germany.

Wu, Y.M. and Kanamori, H. (2005), "Rapid assessment of damage potential of earthquakes in Taiwan from the beginning of P waves", *Bull. Seismol. Soc. Am.*, **95**(3), 1181-1185. https://doi.org/10.1785/0120040193.

Wu, Y.M. and Li, Zhao (2006), "Magnitude estimation using the first three seconds P-wave amplitude in earthquake early warning", *Geophys. Res. Lett.*, **33**(16). https://doi.org/10.1029/2006GL026871.

Zhang, X., Liang, D., Zeng, J. and Lu, J. (2014), "SVR model reconstruction for the reliability of FBG sensor network based on the CFRP impact monitoring", *Smart Struct. Syst.*, **14**(2), 145-158. https://doi.org/10.12989/sss.2014.14.2.145.

AT